Journal of
Materials Chemistry A

Accepted Manuscript

This article can be cited before page numbers have been issued, to do this please use: H. Choi, S. Park, S. Paek, P. Ekanayake, N. Mohammad K. and J. Ko, *J. Mater. Chem. A*, 2014, DOI: 10.1039/C4TA04179H.

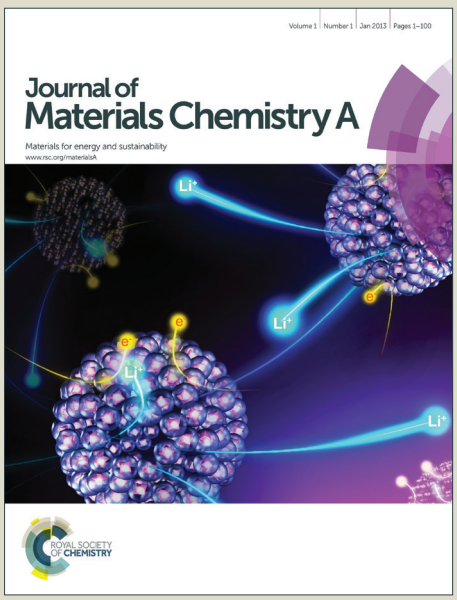

This is an *Accepted Manuscript*, which has been through the Royal Society of Chemistry peer review process and has been accepted for publication.

Accepted Manuscripts are published online shortly after acceptance, before technical editing, formatting and proof reading. Using this free service, authors can make their results available to the community, in citable form, before we publish the edited article. We will replace this *Accepted Manuscript* with the edited and formatted *Advance Article* as soon as it is available.

You can find more information about *Accepted Manuscripts* in the Information for Authors.

Please note that technical editing may introduce minor changes to the text and/or graphics, which may alter content. The journal's standard Terms & Conditions and the Ethical guidelines still apply. In no event shall the Royal Society of Chemistry be held responsible for any errors or omissions in this *Accepted Manuscript* or any consequences arising from the use of any information it contains.

ROYAL SOCIETY OF CHEMISTRY

www.rsc.org/materialsA

Journal of Materials Chemistry A

Dynamic Article Links ►
View Article Online
DOI: 10.1039/C4TA04179H

Cite this: DOI: 10.1039/c0xx00000x

www.rsc.org/xxxxxx

ARTICLE TYPE

Efficient Star-Shaped Hole Transporting Materials with Diphenylethenyl Side Arms for an Efficient Perovskite Solar Cell

Hyeju Choi,[a] Sojin Park,[a] Sanghyun Paek,[a] Piyasiri Ekanayake,[b] Mohammad Khaja Nazeeruddin,[c] Jaejung Ko[a]*

Received (in XXX, XXX) Xth XXXXXXXXX 20XX, Accepted Xth XXXXXXXXX 20XX
DOI: 10.1039/b000000x

Two symmetrical star-shaped hole transporting material (HTMs), *i.e.* **FA-MeOPh** and **TPA-MeOPh** with a fused triphenylamine or triphenylamine core and diphenylethenyl side arms were synthesized. **FA-MeOPh** showed a strong molar absorption coefficient and a red-shifted absorption compared with **TPA-MeOPh** due to its planar configuration. The power conversion efficiency (PCE) of the perovskite solar cells based on **FA-MeOPh** and **TPA-MeOPh** is about 11.86 and 10.79%, in which the efficiency of former is comparable to that (12.75%) of **spiro-OMeTAD** based cell. The high photocurrent (18.39 $mAcm^{-2}$) of **FA-MeOPh** based solar cell relative to **TPA-MeOPh** based one may be attributable to the enhanced absorption in the near-IR region for *mp*-TiO_2/$CH_3NH_3PbI_3$/HTM based cell. The high mobility and low series resistance of *mp*-TiO_2/$CH_3NH_3PbI_3$/**FA-MeOPh** based cell led to the high fill factor (0.698) of **FA-MeOPh** based solar cell relative to **TPA-MeOPh** based one (0.627). In addition, the **FA-MeOPh** based cell showed a relative stability under light soaking for 250 h. The high efficiency, relative stability, synthetically simple and inexpensive materials as the HTMs hold promise to replace the expensive **spiro-OMeTAD**.

Introduction

The organometal halide perovskite $CH_3NH_3PbX_3$ (X = Cl, Br, I) has attracted great attention as light absorbers due to their direct band gap, large optical absorption, high carrier mobility and good stability.[1] Since the first publication on organolead halide perovskite as light absorber in liquid based solar cells with power conversion efficiency of 3.81% for $CH_3NH_3PbI_3$ by Miyasaka,[2] the past few years have witnessed unprecedent rapid development in the perovskite based solar cells.[3] In these cells, the hole transporting material (HTM) is the key component. An impressive photovoltaic performance was achieved over 15% power conversion efficiency with 2,2',7,7'-tetrakis(*N*,*N*-di-*p*-methoxyphenylamine)-9,9'-spirobifluorene (spiro-OMeTAD) as the hole transporting material (HTM) using an one-step precursor deposition,[4] a sequential deposition method,[5] and a dual-source vapor deposition.[6] Alternate small molecule HTMs such as 3,4-ethylenedioxyhtiophene-,[7] pyrene-[8] linear π-conjugated-,[9] butadiene-,[10] spiro-OMeTAD derivative-,[11] and star-shaped[12] based HTMs gave high conversion efficiencies of 11~16%. Some polymer HTMs[13] with excellent electrical properties also gave high photovoltaic performances. Although the best result has been achieved using spiro-OMeTAD as the HTM, the expensive synthetic cost and low-charge carrier mobility of spiro-OMeTAD limit its potential for application of hybrid perovskite solar cells. Therefore, the development of efficient and inexpensive small molecule HTMs with optimal electronic properties remains an attractive goal. One of candidates for such HTMs is the star-shaped triphenylamines, which have been known as HTMs for the active layer of OFETs[14] and OLEDs.[15] Recently, Getautis, *et. al.*[16] have reported the star-shaped charge-transporting materials with a triphenyl core and a number of diphenylethenyl side arms, demonstrating very good hole-transporting mobility. We[13] developed an efficient perovskite solar cell using planar triphenylamine hole conductors.

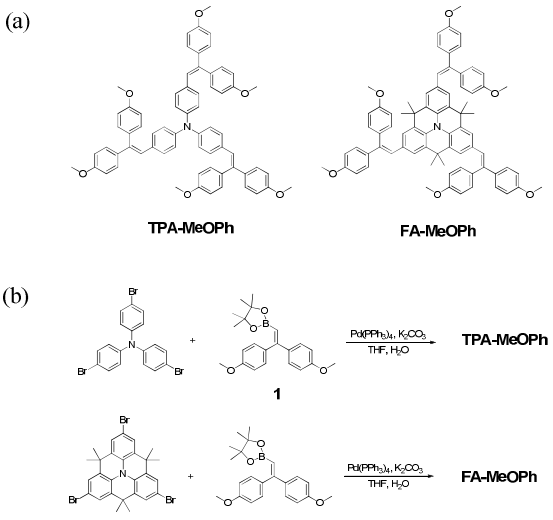

Fig. 1 (a) Chemical structures of **TPA-MeOPh** and **FA-MeOPh**. (b) Schematic diagram for the synthesis of the **TPA-MeOPh** and **FA-MeOPh**.

View Article Online
DOI: 10.1039/C4TA04179H

Herein, we report two types of hole transporting materials incorporated by a planar amine of star-shaped triphenylamine derivative, coded as TPA-MeOPh and FA-MeOPh, and their application in perovskite solar cells. The molecular structure is shown in Figure 1a.

Result and discussion

The synthetic scheme for the preparation of tris{bis(4-methoxyphenylethenyl)-*N*-phenyl}amine (**TPA-MeOPh**)[16] and tris{bis(4-methoxyphenylethenyl)-*N*-phenyl}amine quinolizino acridine (**FA-MeOPh**) is shown in Figure 1b. Detailed synthetic procedures are provided in the experimental section. The hole transporting material **TPA-MeOPh** was synthesized via one step process using inexpensive tris(4-bromophenyl)amine and diphenylethyl borolane. The Suzuki coupling reaction[17] of tris(4-bromophenyl)amine and tribromo-quinolizino acridine with 2-(2,2-bis(4-methoxyphenyl)ethenyl)-4,4,5,5-tetramethyl-1,3,2-dioxaborolane yielded **TPA-MeOPh** and **FA-MeOPh** in ~50% yield. The analytical and spectroscopic data of both HTMs are consistent with the formulated structures.

The UV-vis spectra of **TPA-MeOPh** and **FA-MeOPh** measured in chlorobenzene are shown in the insert of Figure 2a summarized in Table 1. The absorption spectrum of **TPA-MeOPh** exhibits an intense peak at 396 nm. The λ_{max} of **FA-MeOPh** (414 nm) red-shifted (18 nm) relative to that of **TPA-MeOPh** was attributed to the more planar configuration in **FA-MeOPh**, as compared with the more twist (48.9°) between the core nitrogen and phenyl unit in **TPA-MeOPh**. Absorption coefficiency in **FA-MeOPh** increases quite noticeably compared with that of **TPA-MeOPh**, indicating that the transition is accompanied by a big change in the electronic charge distribution through the all conjugated system upon excitation. The fluorescence spectrum of **FA-MeOPh** exhibits a maximum emission at 488 nm with a small Stoke's shift of 74 nm relative to a Stoke's shift of 86 nm, demonstrating that a small structure change in the excited state occurs in **FA-MeOPh** and **TPA-MeOPh** due to a rigid configuration. Figure 2a shows the absorption spectra of two HTMs processed on the perovskite-coated TiO_2 films. Two HTMs-coated films exhibit an enhanced absorption bands due to the superposed absorption characteristics of their constituents.

Figure 2b shows the energy level diagram of the corresponding components in the device. The energy levels of HTMs were determined by ultraviolet photoelectron spectroscopy (UPS) and cyclic voltammetry. The HOMO levels of **TPA-MeOPh** and **FA-MeOPh** are measured to be -5.29 and -5.15 eV, respectively, which have a suitable energy level with the $CH_3NH_3PbI_3$ (-5.43 eV).

Table 1. Photophysical and electrochemical data of HTMs

HTM	λ_{abs}[a]/nm (ε/$M^{-1}cm^{-1}$)	λ_{PL}[a]/nm	HOMO[b] (eV)	LUMO[c] (eV)	E_{gap}[d] (eV)
FA-MeOPh	414 (93 900)	488	-5.15	-2.45	2.70
TPA-MeOPh	396 (71 500)	480	-5.29	-2.59	2.70

[a] UV-vis absorption spectra and fluorescence spectra were measured in Chlorobenzene solution. [b] Redox potential of the compounds were measured in CH_2Cl_2 with 0.1 M (n-$C_4H_9)_4NPF_6$ with a scan rate of 100 mVs^{-1} (*vs*. Fc/Fc^+). [c] $E_{LUMO} = E_{HOMO} + E_{gap}$ [d] E_{gap} was calculated from the absorption thresholds from absorption spectra.

Figure 2c shows the device structure of the hybrid solar cells where fluorine-doped tin oxide glass was deposited with a thin compact layer, followed by deposition of ~260 nm thick mesoporous TiO_2 layer. Perovskite was spin-coated onto the mesoporous TiO_2 film. The HTM was introduced by spin-coating on the m-TiO_2/$CH_3NH_3PbI_3$ film and a 60 nm thick Au layer was finally evaporated at the back contact. The cross-sectional scanning electron microscopy (SEM) images shown in the Figure 2d show the formation of a well-defined hybrid structure with clear interfaces. The thickness of TiO_2, perovskite and HTM layer is ~260, 140, and 150 nm, respectively.

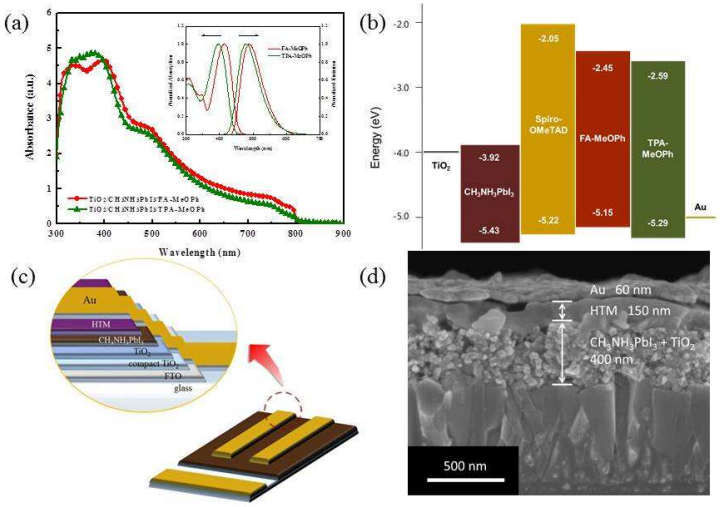

Fig. 2 (a) UV-vis absorption spectra of HTMs coated on mp-TiO_2 and mp-TiO_2/$MAPbI_3$ films. Insert : absorption and emission spectra of the HTMs in chlorobenzene. (b) Energy level diagram of each component. (c) Schematics of the whole device. (d) Scanning electron microscopy (SEM) picture of the cross section of the mp-TiO_2/$MAPbI_3$/HTMs/Au.

View Article Online
DOI: 10.1039/C4TA04179H

Figure 3a shows photocurrent density-voltage (*J-V*) curves for three devices. The corresponding photovoltaic parameters are summarized in Table 2. For a comparative analysis, a reference cell with **spiro-OMeTAD** as HTM was fabricated. As the perovskite solar cells have exhibited a remarkable enhancement in photovoltaic conversion efficiency (PCE) by increasing the conductivity of HTMs via doping the additives such as 4-*tert*-butylpyridine (*t*-Bp) and lithium bis(trifluoromethane-sulfonyl)imide (Li-TFSI) into the HTM[18], we fabricated the cells by doping the two additives into **TPA-MeOPh** or **FA-MeOPh** hole conductor. The **TPA-MeOPh** based cell gave a short-circuit current density (J_{sc}) of 17.33 mAcm^{-2}, an open-circuit voltage (V_{oc}) of 0.99 V, and a fill factor (*ff*) of 0.63, leading to a PCE of 10.79%. Under the similar condition, the **FA-MeOPh** and **spiro-OMeTAD** based cells gave a J_{sc} of 18.39 and 19.87 mAcm^{-2}, a V_{oc} of 0.92 and 0.89 V and a *ff* of 0.70 and 0.72, affording a PCE of 11.86 and 12.75%, respectively. From the photovoltaic performances (Table 2), we have observed that the η value (11.86%) of **FA-MeOPh** based cell is higher than that (10.79%) of **TPA-MeOPh** based one due to a high photocurrent and fill factor. However, The V_{oc} in **TPA-MeOPh** based cell is higher than that of **FA-MeOPh** or **spiro-OMeTAD** based one. As the open-circuit voltage (V_{oc}) is determined by the difference between the quasi-Fermi levels of the TiO_2 and the HOMO of HTM, the higher open-circuit voltage in **TPA-MeOPh** based ell is in good agreement with the relative difference in the HOMO levels of two HTMs.[19] The high photo-current density (J_{sc}) of **FA-MeOPh** based cell relative to **TPA-MeOPh** based one is attributable to the enhanced and red-shifted absorption of *mp*-TiO_2/$CH_3NH_3PbI_3$/**FA-MeOPh** based cell, which is confirmed by the IPCE spectra. The incident photon-to-current conversion efficiency (IPCE) spectra of the three devices were recorded (Figure 3b). The **FA-MeOPh** and **spiro-OMeTAD** based devices enhanced the photocurrent in the whole visible region between 400 and 750 nm relative to that of **TPA-MeOPh** by improving charge collection/extraction. The integrated photocurrent density of **FA-MeOPh** based cell is 17.98 mAcm^{-2}, which is in good agreement with the measured photocurrent density of 18.39 mAcm^{-2} at the standard solar AM 1.5G. In addition, the fill factor of **FA-MeOPh** or **spiro-OMeTAD** based cell is higher than that of **TPA-MeOPh** based cell.

In solar cells, the series resistance (R_s) and hole mobility are related to the fill factor. The series resistance is measured by the slope of the *J-V* curve near V_{oc}. The R_s valud of **FA-MeOPh** and **TPA-MeOPh**, and **spiro-OMeTAD** based cell are calculated to be 36.48, 68.72, and 28.24 Ωcm^{-2}, respectively, in which the lower value of R_s in the **FA-MeOPh** results in higher fill factor. We also measured the hole mobility of HTMs from the space charge limitation of current (SCLC) *J-V* characteristic to check the effect of hole mobility on the fill factor. The hole mobility of **FA-MeOPh**, **TPA-MeOPh**, and **spiro-OMeTAD** evaluated using the Mott-Gurney law[20] was measured to be 4.92 × 10^{-4}, 1.06 × 10^{-4}, and 5.21 × 10^{-4} cm^2/Vs, respectively. The high hole mobility of the **FA-MeOPh** based cell compared with **TPA-MeOPh** based on led to an improved fill factor. Therefore, the fill factor of the devices followed a trend that is closely related to the value of high mobility and low series resistance.

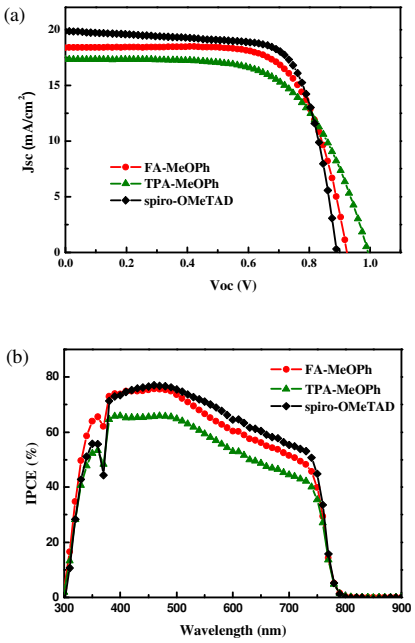

Fig. 3 (a) Photocurrent-voltage (*J-V*) characteristics of the solar cells with **FA-MeOPh** (●), **TPA-MeOPh** (▲) and **spiro-OMeTAD** (◆) under AM 1.5 conditions (100 mW/cm^2). (b) Corresponding IPCE spectra.

Table 2. Summary of photovoltaic parameters derived from *J-V* measurements of $CH_3NH_3PbI_3$ based devices.

HTMs	J_{sc} (mAcm^{-2})	V_{oc} (V)	*ff*	η (%)
FA-MeOPh[a]	18.39	0.924	0.698	11.86
FA-MeOPh[b]	16.97	0.907	0.596	9.18
TPA-MeOPh[a]	17.33	0.994	0.627	10.79
TPA-MeOPh[b]	15.01	0.940	0.528	7.45
Spiro-OMeTAD[a]	19.87	0.890	0.721	12.75

Performances of DSSCs were measured with a metal mask of 0.16 cm^2 working area. Voltage Settling Time: 40ms. [a]Addition of *t*-Bp and LiTFSI as additives. [b]Without any additives.

Since the long-term stability is very critical for sustained cell operation, we carried out long-term aging test. Figure 4 shows the photovoltaic performance during long-term light soaking tests of **FA-MeOPh**, **TPA-MeOPh**, and **spiro-OMeTAD** based solar cells. After 250 h of aging, the initial efficiency of 11.24% in the **FA-MeOPh** based cell decreased to 8.42%, giving a 25.1% reduction. On the other hand, the initial efficiency of 10.12% in the **TPA-MeOPh** based cell sharply decreased to 5.84%, giving a 42.3% reduction. During the aging test of both devices, the V_{oc} and *ff* remains almost constant. However, the J_{sc} of **FA-MeOPh** and **TPA-MeOPh** based cells sharply decreased by 4.08 mAcm^{-2} and 7.74 mAcm^{-2}, respectively, due to the contamination of water. In addition, the relative stability of the **FA-MeOPh** based cell compared with the **TPA-MeOPh** based one may be attributable to the tight packing of the former on the $CH_3NH_3PbI_3$ layer due to a planar molecular configuration.

View Article Online
DOI: 10.1039/C4TA04179H

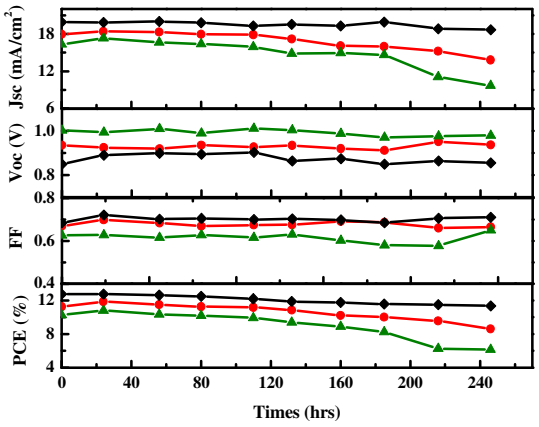

Fig. 4 Stability test for devices based on **FA-MeOPh** (●), **TPA-MePh** (▲) and **spiro-OMeTAD** (◆) in air at room temperature under one sun illumination.

Experimental

General methods

Solvents were distilled from appropriate reagents. All reagents were purchased from Sigma-Aldrich, Acros and TCI. Tribromo-triarylamine,[21] and 2-(2,2-bis(4-methoxyphenyl)vinyl)-4,4,5,5-tetramethyl-1,3,2-dioxaborolane **1**[22] were prepared according to the literature procedure. ^{1}H and ^{13}C NMR spectra were recorded on a Varian Mercury 300 spectrometer. Chemical shifts δ were calibrated against TMS as an internal standard. Elemental analyses were performed with a Carlo Elba Instruments CHNS-O EA 1108 analyzer. The absorption and photoluminescence spectra were recorded on a Perkin-Elmer Lambda 2S UV-visible spectrometer and a Perkin LS fluorescence spectrometer, respectively. CV of the **FA-MeOPh** and **TPA-MeOPh** was measured in dichloromethane solution with 0.1 M tetrabutyl ammonium hexafluorophosphate (n-Bu_4NPF_6) as the supporting salt. The platinum working electrode consisted of a platinum wire sealed in a soft glass tube with a surface of 0.785 mm^2, which was polished down to 0.5 μm with Buehler polishing paste prior to use in order to obtain reproducible surfaces. The counter electrode consisted of a platinum wire and the reference electrode was an Ag/AgCl secondary electrode.

Solar Cell Fabrication

FTO glass plates (Pilkington, TEC-8) were cleaned in a detergent solution using an ultrasonic bath for 30 min, rinsed with water and ethanol. The compact TiO_2 layer was deposited on the etched F-doped tin oxide substrate by spray pyrolysis at 450 °C, using titanium diisopropoxide bis(acetylacetonate) solution. The FTO glass plates were immersed in 40 mM $TiCl_4$ (aqueous) at 70 °C for 30 min and sintered at 500 °C for 30 min. Mesoporous TiO_2 films was deposited by spin coating of a diluted TiO_2 paste (Dyesol 18NR-T, 1:3.5w/w diluted with ethanol) at 5000 rpm for 30 s. The films were sintered at 500 °C. The PbI_2 in DMF solution (1.0 M) was dropped on the TiO_2/FTO substrate by spin-coating at 6500 rpm for 30 s, and dried on a hot plate at 70 °C for 30 min. After cooling down, the film was dipped into a CH_3NH_3I/2-propanol solution (8 mg/mL) for 25 s, and dried at 70 °C for 15 min. For a deposition of HTM layers, **FA-MeOPh**/chlorobenzene (35 mM), **TPA-MeOPh**/chlorobenzene (35 mM) and spiro-OMeTAD/chlorobenzene (60 mM) solutions were prepared with two additives. 7.0 μL Li-TFSI (Li-bis(trifluoromethanesulfonyl)imide)/acetonitrile (520 mg/1 mL) and 8.0 μL TBP (4-*tert*-butylpyridine) were added to the HTM/chlorobenzene solutions as additives. The HTMs were spin-cast on top of the $CH_3NH_3PbI_3/TiO_2$/ FTO substrate at 3000 rpm. Finally, the device was pumped down to lower than 10^{-5} torr and a ~60 nm thick Au counter electrode was deposited on top.

Measurement

Solar cells efficiencies were characterized under simulated 100 mW/cm^2 AM 1.5G irradiation from a Xe arc lamp with an AM 1.5 global filter. Simulator irradiance was characterized using a calibrated spectrometer and illumination intensity was set using an NREL certified silicon diode with an integrated KG1 optical filter: spectral mismatch factors were calculated for each device in this report to be less than 5%. Short circuit currents were also found to be with 5% of values calculated using the integrated external quantum efficiency (EQE) spectra and the solar spectrum. The EQE was measured by underfilling the device area using a reflective microscope objective to focus the light output from a 75 watt Xe lamp, monochromator, and optical chopper; photocurrent was measured using a lock-in amplifier and the absolute photon flux was determined by a calibrated silicon photodiode.

TPA-MeOPh. A mixture of boron compound **1** (1.09 g, 2.97 mmol), tris(4-bromophenyl)amine (0.32 g, 0.66 mmol), tetrakis(triphenylphosphine)palladium(0) (0.10 g, 0.086 mmol) and potassium carbonate solution (0.63 g, 4.56 mmol) in dry tetrahydrofuran (12 mL) and H_2O (3 mL) was refluxed overnight. The mixture was cooled to room temperature and extracted with diethyl ether (3×50 mL) and the extracts were washed with brine and dried ($MgSO_4$). The solvent was removed *in vacuo* and the residue was purified by column chromatography on silicagel eluting with CH_2Cl_2/Hexane (1:4) to give **TPA-MeOPh**. The analytical data of **TPA-MeOPh** were consistent with previous literature (ref 16).

FA-MeOPh. The product **FA-MeOPh** was prepared using the same procedures for compound **TPA-MeOPh** except that fused tribromoarylamine (1.79 g, 2.97 mmol) were used instead of tris(4-bromophenyl)amine. ^{1}H NMR (300 MHz, $CDCl_3$): δ 7.45 (s, 6H), 7.28 (d, J = 8.4 Hz, 12H), 6.86 (d, J = 8.4 Hz, 12H), 5.30 (s, 3H), 3.83 (s, 18H), 1.57 (s, 18H). ^{13}C NMR (75 MHz, $CDCl_3$): δ 159.1, 158.9, 139.9, 136.6, 133.5, 132.1, 131.7, 129.7, 129.4, 128.6, 126.2, 125.4, 114.6, 113.7, 55.5, 55.4, 35.2, 33.2. MS: *m/z* 1079.51 [M$^+$]. Anal. Calc. for $C_{75}H_{69}NO_6$: C, 83.38; H, 6.44. Found : C,83.22; H, 6.36.

Conclusions

We synthesized two efficient transporting materials with a fused triphenylamine or triphenylamine core and diphenylethyenyl side arms. The photovoltaic performance is quite sensitive to the structural modification of HTMs. The perovskite based cell using **FA-MeOPh** as a HTM gave an overall conversion efficiency of

View Article Online
DOI: 10.1039/C4TA04179H

11.86%, showing a competitive photovoltaic performance to the **spiro-OMeTAD** based cell (12.75%). Moreover, the **FA-MeOPh** based cell stored for 250 h without any encapsulation showed a relative stability. This novel and high-performing HTMs offers a new design strategy toward developing efficient HTMs comparable to the **sprio-OMeTAD** for photovoltaic applications and studies directed this goal are now in progress.

Acknowledgements

This work was supported by the International Science and Business Belt Program through the Ministry of Science, ICT and Future Planning (No. 2012K001573), and the National Research Foundation of Korea (NRF) grant funded by the Korea government (MSIP) (2014R1A2A2A03004716).

Notes and references

[a] *Department of Advanced Material Chemistry, Korea University, 2511, Sejong-ro, Jochiwon-eup, Sejong City 339-700, Republic of Korea. Fax: 82 41 860 1331; Tel: 82 41 860 1337; E-mail: jko@korea.ac.kr*
[b] *Applied Physics Program, Faculty of Science, University of Brunei Darussalam, Jalan Tungku Link, Gadong BE 1410, BRUNEI DARUSSALAM.*
[c] *Laboratory of Photonics and Interfaces, Department of Chemistry and Chemical Engineering, Swiss Federal Institute of Technology, Station 6, CH-1015 Lausanne, Switzerland.*

1 a) H.-S. Kim, C.-R. Lee, J.-H. Im, K.-B. Lee, T. Moehl, A. Marchioro, S.-J. Moon, R. Humphry-Baker, J.-H. Yum, J. E. Moser, M. Grätzel, N.-G. Park, *Sci. Rep*. 2012, **2**, 591; b) J.-H. Yum, C.-R. Lee, J.-W. Lee, S.-W. Park, N.-G. Park, *Nanoscale*, 2011, **3**, 4088.
2 A. Kojima, K. Teshima, Y. Shirai and T. Miyasaka, *J. Am. Chem. Soc*., 2009, **131**, 6050.
3 a) M. A. Green, A. Ho-Baillie and H. J. Snaith, *Nature Photonics*, 2014, **8**, 506; b) P. Gao, M. Grätzel and M. K. Nazeeruddin, *Energy Environ. Sci*., 2014, **7**, 2448.
4 K. Wojciechowski, M. Saliba, T. Leijtens, A. Abate and H. J. Snaith, *Energy Environ. Sci.*, 2014, **7**, 1142.
5 J. Burschka, N. Pellet, S.-J. Moon, R. Humphry-Baker, P. Gao, M. K. Nazeeruddin, M. Grätzel, *Nature*, 2013, **499**, 316.
6 M. Liu, M. B. Johnston, H. J. Snaith, *Nature*, 2013, **501**, 395.
7 H. Li, K. Fu, A. Hagfeldt, M. Grätzel, S. G. Mhaisalkar, A. C. Grimsdale, *Angew. Chem. Int. Ed*. 2014, **53**, 4085.
8 N. J. Jeon, J. Lee, J. H. Noh, M. K. Nazeeruddin, M. Grätzel, S. I. Seok, *J. Am. Chem. Soc*. 2013, **135**, 19087.
9 J. Wang, S. Wang, X. Li, L. Zhu, Q. Meng, Y. Xiao and D. Li, *Chem. Commun*., 2014, **50**, 5829.
10 S. Lv, L. Han, J. Xiao, L. Zhu, J. Shi, H. Wei, Y. Xu, J. Dong, X. Xu, D. Li, S. Wang, Y. Luo, Q. Meng and X. Li, *Chem. Commun*., 2014, **50**, 6931.
11 N. J. Jeon, H. G. Lee, Y. C. Kim, J. Seo, J. H. Noh, J. Lee and S. I. Seok, *J. Am. Chem. Soc*., 2014, **136**, 7837.
12 P. Qin, S. Peak, M. I. Dar, N. Pellet, J. Ko, M. Grätzel and M. K. Nazeeruddin, *J. Am. Chem. Soc.*, 2014, **136**, 8516.
13 (a) J. H. Heo, S. H. Im, J. H. Noh, T. N. Mandal, C.-S. Lim, J. A. Chang, Y. H. Lee, H.-J. Kim, A. Sarkar, M. K. Nazeeruddin, M. Grätzel, S. I. Seok, *Nature Photonics*, 2013, **7**, 486; (b) Y. S. Kwon, J. Lim, H.-J. Yum, Y.-H. Kim, T. Park, *Energy Environ. Sci*., 2014, **7**, 1454; (c) J. M. Ball, M. M. Lee, A. Hey and H. J. Snaith, *Energy Environ. Sci*., 2013, **6**, 1739; (d) B. Walker, J. H. Liu, C. Kim, G. C. Welch, J. K. Park, J. Lin, P. Zalar, C. M. Proctor, J. H. Seo, G. C. Bazan, and T.-Q. Nguyen, *Energy Environ. Sci*., 2013, **6**, 952; (e) H. Bronstein, Z. Chen, R. S. Ashraf, W. Zhang, J. Du, J. R. Durrant, P. S. Tuladhar, K. Song, S. E. Watkins, Y. Geerts, M. M. Wienk, R. A. J. Janssen, T. Anthopoulos, H. Sirringhaus, M. Heeney and I. McCulloch, *J. Am. Chem. Soc*., 2011, **133**, 3272.
14 S. Allard, B. Forster, B. Souharce, H. Thiem and U. Scherf, *Angew. Chem. Int. Ed*., 2008, **47**, 4070
15 P. Strohriegl and J. V. Grazulevicius, *Adv. Mater*., 2002, **14**, 1439.
16 T. Malinauskas, M. daskeviciene, G. Bubniene, I. Petrikyte, S. Raisys, K. Kazlauskas, V. Gaidelis, V. Jankauskas, R. Maldzius, S. Jursenas and V. Getautis, *Chem. Eur. J*. 2013, **19**, 15044.
17 (a) C.-H. Huang, N. D. McClenaghan, A. Kuhn, J. W. Hofstraat, D. M. Bassani, *Org. Lett*., 2005, **7**, 3409; (b) K. J. Hoffmann, E. Bakken, E. J. Samuelsen and P. H. J. Carlsen, *Synth. Metal*, 2000, **113**, 3944.
18 J. Burschka, A. Dualeh, F. Kessler, E. Baranoff, N.-L. Cevey-Ha, C. Yi, M. K. Nazeeruddin, M. Grätzel, *J. Am. Chem. Soc*., 2011, **133**, 18042.
19 P. Wang, S. M. Zakeeruddin, J.-E. Moser and M. Grätzel, *J. Phys. Chem. B*, 2003, **107**, 13280.
20 V. D. Mihailetchi, H. Xie, B. de Boer, L. J. A. Koster, P. W. M. Blom, *Adv. Funct. Mater.* 2006, **16**, 699.
21 Z. Fang, V. Chellappan, R. D. Webster, L. Ke, T. Zhang, B. Liu and Y.-H. Lai, *J. Mater. Chem*., 2012, **22**, 15397.
22 K. Itami, K. Tonogaki, Y. Ohashi, and J.-I. Yoshida, *Org. Lett*., 2004, **6**, 4093.

View Article Online
DOI: 10.1039/C4TA04179H

Efficient Star-Shaped Hole Transporting Materials with Diphenylethenyl Side Arms for an Efficient Perovskite Solar Cell

Hyeju Choi, Sojin Park, Sanghyun Paek, Piyasiri Ekanayake, Mohammad Khaja Nazeeruddin, Jaejung Ko

This paper describes the synthesis of two novel symmetrical star-shaped hole transporting material (HTMs) possessing a fused triphenylamine or triphenylamine core and diphenylethenyl side arms. A fused triphenylamine play a key role in strong molar absorption coefficient and a red-shifted absorption, which resulted in a significant improvement in both the short-circuit photocurrent density (J_{sc}) and overall conversion efficiency.